

基于EPR导引的连续变量安全量子克隆

王俊¹,翟淑琴^{1,2*}¹山西大学物理电子工程学院,山西太原030006;²山西大学光电研究所量子光学与光量子器件国家重点实验室,山西太原030006

摘要 利用量子信道和经典信道相结合的方法,采用部分脱体传输设计了连续变量 $1 \rightarrow 2$ 量子克隆方案,在此基础上研究了克隆保真度与EPR导引之间的关系。研究结果表明:双向量子导引态是实现相干态安全量子克隆的必要资源。对于克隆输出模Clone 1,取最优增益时克隆保真度超过不可克隆阈值的实现需要共享纠缠源的双向导引,但并不是所有双向导引的资源都能使克隆的保真度大于 $\frac{2}{3}$ 。在输出模Clone 1的最优增益下,观察了输出模Clone 1和输出模Clone 2的保真度随分束器反射率和压缩参数的变化,发现使用纠缠度较小但可导引的资源可以实现较高的克隆保真度,且克隆过程中也不需要较高的反射率。此研究结果对安全量子通信网络的构建具有一定的参考意义。

关键词 量子光学;量子克隆;量子关联;双向导引

中图分类号 O437

文献标志码 A

DOI: 10.3788/AOS231278

1 引言

1935年,Einstein、Podolsky 和 Rosen^[1]以量子力学基本原理为基础提出了著名的EPR佯谬,推断出与经典理论物理实在论相矛盾的结论,他们把这一特性称为“幽灵般的超距作用”。1935年,薛定谔在研究EPR佯谬时提出了EPR导引的概念^[2]。1989年,Reid^[3]提出了量子导引的定性判据,Alice和Bob共享一对量子态,若Alice可以通过自己的测量结果来推断Bob的测量结果,则可以实现Alice对Bob的导引。2007年,Jones、Wiseman和Doherty^[4]根据违背局域隐变量模型给出了量子导引的严格定义,描述了对一个粒子的局部测量能够非局域地影响另一个粒子的能力,其测量结果无法用局域隐变量模型来解释,并且指出导引是介于贝尔非局域性和纠缠之间特殊的量子关联,它具有天然的不对称性^[5-8]和单配性^[9-10],这些独特的性质使得量子导引成为多种量子信息过程中的重要资源。在单端设备无关的量子密钥分发^[11-12]、安全量子离物传态^[13-14]和子信道识别^[15]的任务中,利用量子导引可以提高获取密钥的速率、提高协议的效率以及安全性。因此,研究量子导引在量子通信过程中的作用具有十分重要的意义。

量子隐形传态和量子克隆作为量子信息和量子通信中的重要协议,在量子纠缠和经典通信的帮助下可

以实现任意未知量子态从一个位置传输到另外一个位置。量子力学的基本原理限制了对一个量子态的完美克隆,即不可克隆原理^[16-18]。通常情况下量子克隆有两种实现方案,分别为分离变量系统和连续变量系统,其中分离变量系统通常描述的是光子的偏振^[19-21]或轨道角动量^[22-23]编码的量子态,而连续变量系统通常描述的是光场的正交振幅和正交相位^[24]编码的量子态。目前,连续变量 $1 \rightarrow M$ 相干态的量子克隆在理论^[25]和实验上^[26-28]都得到了广泛的研究。2000年,Cerf等提出了连续变量高斯态的量子克隆,并给出了 $\frac{2}{3}$ 的量子克隆保真度边界;2001年,Grangier课题组^[29]在海森堡表象下给出了相干态连续变量量子克隆(离物传态)的量子和经典保真度边界。2004年,Furusawa课题组^[30]利用3个单模OPO获得最佳保真度为0.64的连续变量量子离物传态网络;2012年,潘建伟课题组^[31]在实验上实现了远距离的量子隐形传态;2018年,Wang等^[32]研究了利用部分纠缠的GHZ态的隐形传态;2020年,Guo等^[33]发现信道中的纠缠退相干使得量子隐形传态的保真度降低;2022年,荆杰泰课题组^[34]全面介绍了兼容全光量子隐形传态、部分脱体量子态传输和量子克隆协议的平台;2023年,邢磊等^[35]提出了通过超纠缠交换的方法提高量子克隆保真度的方案。综上所述,突破不可克隆极限并实现量子态非经

收稿日期:2023-07-18;修回日期:2023-09-22;录用日期:2023-10-10;网络首发日期:2023-11-14

基金项目:山西省自然科学基金(202203021211306)、国家自然科学基金(12074233)、国家重点研发计划(2021YFC2201802)、2022年山西省高等学校教学改革创新项目(J20220082)、山西1331项目

通信作者:^{*}xiaozhai@sxu.edu.cn

典特性的传输仍然是一个挑战。

本文从理论上研究了部分脱体传输的克隆保真度与EPR纠缠源之间的关系。首先,分析了 $1 \rightarrow 2$ 克隆方案中两个输出模的保真度、EPR共享纠缠源的纠缠和导引特性;其次,研究了最优增益下输出模Clone 1的保真度与导引特性之间的关系;最后,在输出模Clone 1的最优增益下,研究了输出模Clone 2的保真度随反射率和压缩参数的变化。

2 导引判据和纠缠判据

2.1 导引判据

若Alice和Bob共享一对量子态,其中Bob在自己的位置上进行测量时可以得到测量结果 \hat{X}_B 和 \hat{P}_B ,若Alice可以通过自己的测量结果 \hat{X}_A 、 \hat{P}_A 来推断Bob的测量结果为 $\hat{X}_B^{(0)} = g_x \hat{X}_A$ 、 $\hat{P}_B^{(0)} = g_p \hat{P}_A$,则 \hat{X}_B 和 $\hat{X}_B^{(0)}$ 、 \hat{P}_B 和 $\hat{P}_B^{(0)}$ 的偏差仅由 $\hat{X}_B - g_x \hat{X}_A$ 、 $\hat{P}_B + g_p \hat{P}_A$ 确定,所以对 \hat{X}_B 、 \hat{P}_B 的平均估计误差分别为 $\Delta_{\text{inf}} \hat{X}_B = \langle [\hat{X}_B - g_x \hat{X}_A] \rangle$ 、 $\Delta_{\text{inf}} \hat{P}_B = \langle [\hat{P}_B + g_p \hat{P}_A] \rangle$ 。通过寻找最佳增益因子可得到 $\Delta_{\text{inf}}^2 \hat{X}_B = \langle [\hat{X}_B - g_x \hat{X}_A]^2 \rangle$ 、 $\Delta_{\text{inf}}^2 \hat{P}_B = \langle [\hat{P}_B + g_p \hat{P}_A]^2 \rangle$ 的最小值;若满足

$$S_{B|A} =$$

$$\Delta(\hat{X}_B - g_x \hat{X}_A) \Delta(\hat{P}_B + g_p \hat{P}_A) < \frac{1}{2} \left| \langle [\hat{X}_B, \hat{P}_B] \rangle \right|, \quad (1)$$

则Alice可以导引Bob,其中 g_x 和 g_p 为增益因子^[3]。当Alice可以导引Bob,而Bob不能导引Alice时,即表现为量子导引的单向性,量子导引的单向性来自两个子系统间天然的不对称性。

2.2 纠缠判据

若Alice和Bob共享一对纠缠态,二者之间的纠缠可以用以下判据^[36-37]来证明:

$$E_{\text{ent}} = \frac{\Delta(\hat{X}_B - g_x \hat{X}_A) \cdot \Delta(\hat{P}_B + g_p \hat{P}_A)}{1 + g_x g_p} < 1, \quad (2)$$

式中: E_{ent} 为两个系统之间的纠缠度。Alice和Bob之间的最大纠缠对应于 E_{ent} 的值趋向于0。

3 量子导引条件下的 $1 \rightarrow 2$ 量子克隆

图1所示为量子导引条件下的部分脱体 $1 \rightarrow 2$ 量子克隆方案。Alice将输入相干态分成两部分,其中一部分与纠缠EPR光束中的一束进行贝尔态测量,测量结果调制到未被破坏的部分,并对未被破坏部分进行平移后传输至Bob端。Bob在另一束纠缠EPR光束的帮助下完成对初始量子态的克隆。

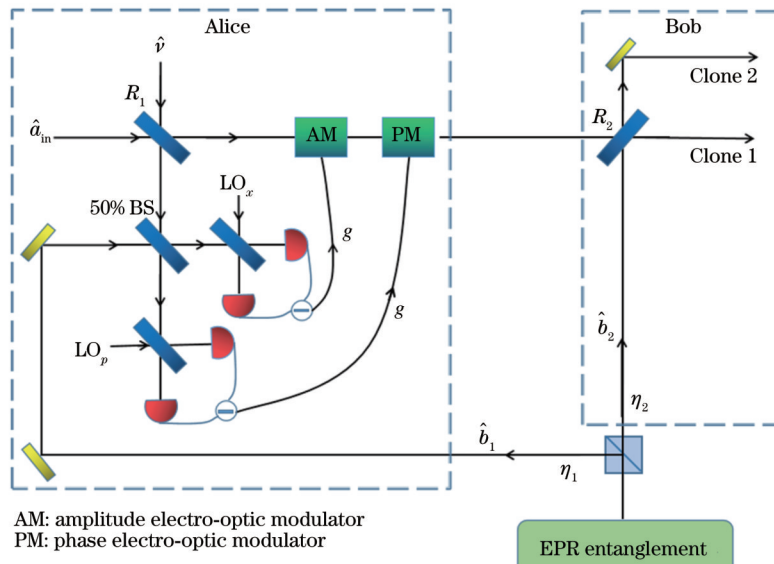


图1 量子导引条件下的 $1 \rightarrow 2$ 量子克隆模型

Fig. 1 $1 \rightarrow 2$ quantum cloning model under quantum steering conditions

Alice和Bob共享一对EPR纠缠源,该纠缠源可以由一对振幅压缩态和相位压缩态在50:50分束器上耦合得到,初始的两个压缩态可以表示为

$$\begin{cases} \hat{e}_1 = \frac{1}{2} (e^r \hat{X}_1^{(0)} + i e^{-r} \hat{P}_1^{(0)}) \\ \hat{e}_2 = \frac{1}{2} (e^{-r} \hat{X}_2^{(0)} + i e^r \hat{P}_2^{(0)}) \end{cases}, \quad (3)$$

式中: $\hat{X}_i^{(0)}$ 和 $\hat{P}_i^{(0)}$ ($i=1, 2$)分别表示真空态的正交振幅和正交位相; r 为压缩参数。经过损耗通道产生的两束EPR输出光 \hat{b}_1 和 \hat{b}_2 可以表示为

$$\begin{cases} \hat{b}_1 = \sqrt{\frac{\eta_1}{2}} (\hat{e}_1 + \hat{e}_2) + \sqrt{1 - \eta_1} \hat{v}_1 \\ \hat{b}_2 = \sqrt{\frac{\eta_2}{2}} (\hat{e}_1 - \hat{e}_2) + \sqrt{1 - \eta_2} \hat{v}_2 \end{cases}, \quad (4)$$

式中: η_i ($i=1, 2$)为损耗通道的传输效率; $\hat{\nu}_i$ 为由损耗信道引入的真空噪声。

如图1所示,将相干态光场 \hat{a}_{in} 作为输入态, \hat{a}_{in} 算符的表达式为 $\hat{a}_{\text{in}}=\frac{1}{2}(\hat{X}_{\text{in}}+\text{i}\hat{P}_{\text{in}})$ 。Alice将输入态的反射光与纠缠态的 \hat{b}_1 在50:50的分束器上耦合后执行贝尔态测量,并将测量结果通过振幅调制器和相位调制器调制到输入态的透射部分,透射部分光场在调制后发生平移:

$$\hat{a}_{\text{disp}} = \left(\sqrt{1-R_1} + \frac{g}{\sqrt{2}} \sqrt{R_1} \right) \hat{a}_{\text{in}} + \left(\sqrt{R_1} - \frac{g}{\sqrt{2}} \sqrt{1-R_1} \right) \hat{\nu} - \frac{g}{\sqrt{2}} \hat{b}_1^+, \quad (5)$$

式中: R_1 为分束器的反射率; g 为调制因子; $\hat{\nu}$ 为分束器 R_1 引入的真空噪声。

Bob接收到平移光场后与纠缠态的 \hat{b}_2 在反射率为 R_2 的分束器上耦合,产生两个输出模Clone 1 和 Clone 2,完成 $1 \rightarrow 2$ 量子克隆,克隆输出模表示为

$$\begin{cases} \hat{a}_{\text{Clone 1}} = \sqrt{1-R_2} \hat{a}_{\text{disp}} + \sqrt{R_2} \hat{b}_2 \\ \hat{a}_{\text{Clone 2}} = \sqrt{R_2} \hat{a}_{\text{disp}} - \sqrt{1-R_2} \hat{b}_2 \end{cases}. \quad (6)$$

为方便起见,令 $R_1=R_2=R$,利用式(5)及式(6),可以得出克隆输出态Clone 1的正交振幅和正交位相表达式:

$$\begin{aligned} \hat{X}_{\text{Clone 1}} = & \left[(1-R) + \frac{g}{\sqrt{2}} \sqrt{R(1-R)} \right] \hat{X}_{\text{in}} + \\ & \left[\sqrt{R(1-R)} - \frac{g}{\sqrt{2}} (1-R) \right] \hat{X}_{\nu} + \sqrt{R} \left(\hat{X}_{b_2} - \frac{g}{\sqrt{2}} \sqrt{\frac{1-R}{R}} \hat{X}_{b_1} \right), \end{aligned} \quad (7)$$

$$\begin{aligned} \hat{P}_{\text{Clone 1}} = & \left[(1-R) + \frac{g}{\sqrt{2}} \sqrt{R(1-R)} \right] \hat{P}_{\text{in}} + \\ & \left[\sqrt{R(1-R)} - \frac{g}{\sqrt{2}} (1-R) \right] \hat{P}_{\nu} + \sqrt{R} \left(\hat{P}_{b_2} + \frac{g}{\sqrt{2}} \sqrt{\frac{1-R}{R}} \hat{P}_{b_1} \right). \end{aligned} \quad (8)$$

根据导引判据[式(1)],结合式(7)和式(8),在此 $1 \rightarrow 2$ 克隆过程中,定义导引

$$S_{b_2|b_1} = \Delta \left(\hat{X}_{b_2} - \frac{g}{\sqrt{2}} \sqrt{\frac{1-R}{R}} \hat{X}_{b_1} \right) \cdot \Delta \left(\hat{P}_{b_2} + \frac{g}{\sqrt{2}} \sqrt{\frac{1-R}{R}} \hat{P}_{b_1} \right). \quad (9)$$

当 $\eta_1=\eta_2=1$ 时,考虑经典极限($r=0$)情况下,此时 \hat{b}_1 对 \hat{b}_2 的导引关系为

$$S_{b_2|b_1} = 1 + \frac{g^2(1-R)}{2R}, \quad (10)$$

由此建立起纠缠与导引的关系

$$E_{\text{ent. } b_2|b_1} = \frac{S_{b_2|b_1}}{1 + \frac{g^2(1-R)}{2R}} < 1. \quad (11)$$

通过式(11)可以得出纠缠程度最大时对应的最优增益 $g=g_{b_2|b_1}$:

$$g_{b_2|b_1} = \frac{(m-n) + \sqrt{(m-n)^2 + 4c^2}}{\sqrt{2} c \sqrt{\frac{1-R}{R}}}, \quad (12)$$

式中: $n=\langle \hat{X}_{b_1}, \hat{X}_{b_1} \rangle=\eta_1 \cosh(2r)+1-\eta_1$; $m=\langle \hat{X}_{b_2}, \hat{X}_{b_2} \rangle=\eta_2 \cosh(2r)+1-\eta_2$; $c=\langle \hat{X}_{b_1}, \hat{X}_{b_2} \rangle=\sqrt{\eta_1 \eta_2} \sinh(2r)$ 。 $g_{b_2|b_1}$ 的值量化了纠缠资源间的不对称性:当 $\eta_1=\eta_2$ 时,可得 $g_{b_2|b_1}=\sqrt{2}$,纠缠源的 \hat{b}_1 和 \hat{b}_2 之间关系对称;当 $g_{b_2|b_1}>\sqrt{2}$ 时,对应 $\eta_1<\eta_2$,此时 $S_{b_1|b_2} < S_{b_2|b_1}$,即 \hat{b}_2 对 \hat{b}_1 的导引要大于 \hat{b}_1 对 \hat{b}_2 的导引,对于任意高斯纠缠源,都可以实现从Alice到Bob的量子克隆;当 $g_{b_2|b_1}<\sqrt{2}$ 时,对应 $\eta_1>\eta_2$,此时 $S_{b_1|b_2} > S_{b_2|b_1}$,要想实现从Alice到Bob的量子克隆,就需要交换 \hat{b}_1 和 \hat{b}_2 的EPR通道。

对于任意高斯态,量子克隆保真度^[38]为

$$F = \frac{2}{\sqrt{\left\{ 1 + \left[\Delta(\hat{X}_{\text{out}}) \right]^2 \right\} \left\{ 1 + \left[\Delta(\hat{P}_{\text{out}}) \right]^2 \right\}}}, \quad (13)$$

由此可得到克隆输出态Clone 1的保真度为

$$F_1 = \begin{cases} \frac{2}{1 + \left[(1-R) + \frac{g_{b_2|b_1}}{\sqrt{2}} \sqrt{R(1-R)} \right]^2 + \left[\sqrt{R(1-R)} - \frac{g_{b_2|b_1}}{\sqrt{2}} (1-R) \right]^2 + RS_{b_2|b_1}}, & \eta_1 \leqslant \eta_2 \\ \frac{2}{1 + \left[(1-R) + \frac{g_{b_1|b_2}}{\sqrt{2}} \sqrt{R(1-R)} \right]^2 + \left[\sqrt{R(1-R)} - \frac{g_{b_1|b_2}}{\sqrt{2}} (1-R) \right]^2 + RS_{b_1|b_2}}, & \eta_1 > \eta_2 \end{cases}. \quad (14)$$

由以上可得出克隆输出模Clone 1的保真度随 η_1 、 η_2 及纠缠源间导引的变化关系。

同理,可得出克隆输出态Clone 2的保真度表达式:

$$F_2 = \begin{cases} \frac{2}{1 + \left[\sqrt{R(1-R)} + \frac{g_{b_2|b_1}}{\sqrt{2}} R \right]^2 + \left[R - \frac{g_{b_2|b_1}}{\sqrt{2}} \sqrt{R(1-R)} \right]^2 + (1-R) \Delta \left[\hat{X}_{b_2} + \frac{g_{b_2|b_1}}{\sqrt{2}} \sqrt{\frac{R}{1-R}} \hat{X}_{b_1} \right]^2}, & \eta_1 \leq \eta_2 \\ \frac{2}{1 + \left[\sqrt{R(1-R)} + \frac{g_{b_1|b_2}}{\sqrt{2}} R \right]^2 + \left[R - \frac{g_{b_1|b_2}}{\sqrt{2}} \sqrt{R(1-R)} \right]^2 + (1-R) \Delta \left[\hat{X}_{b_1} + \frac{g_{b_1|b_2}}{\sqrt{2}} \sqrt{\frac{R}{1-R}} \hat{X}_{b_2} \right]^2}, & \eta_1 > \eta_2 \end{cases} \quad (15)$$

因此,可以在输出模Clone 1保真度最大的最优增益前提下,研究输出模Clone 2保真度随 η_1 和 η_2 的变化关系。

4 研究结果

4.1 纠缠源 \hat{b}_1 、 \hat{b}_2 之间的导引关系以及最优增益 g_{opt} 随 η_1 和 η_2 的变化

选取 $R=0.5$ 、 $r=1.15$ (对应10 dB),图2(a)、(b)分别表示 \hat{b}_1 对 \hat{b}_2 的导引以及 \hat{b}_2 对 \hat{b}_1 的导引的最小值,可以看到:当且仅当 $\eta_1>0.5$ 时,存在 \hat{b}_1 对 \hat{b}_2 的导引;当且仅当 $\eta_2>0.5$ 时,存在 \hat{b}_2 对 \hat{b}_1 的导引。进而得

到:当 $\eta_1<0.5$ 且 $\eta_2<0.5$ 时, \hat{b}_1 和 \hat{b}_2 之间不存在导引;当 $\eta_1>0.5$ 且 $\eta_2<0.5$ 时,只存在 \hat{b}_1 对 \hat{b}_2 的单向导引;当 $\eta_1<0.5$ 且 $\eta_2>0.5$ 时,只存在 \hat{b}_2 对 \hat{b}_1 的单向导引;当 $\eta_1>0.5$ 且 $\eta_2>0.5$ 时, \hat{b}_1 和 \hat{b}_2 之间存在双向导引。图2(c)所示为在最优增益 g_{opt} 下 \hat{b}_1 和 \hat{b}_2 之间的纠缠,且纠缠的程度随传输效率 η_1 和 η_2 的增大而增强。从图2(d)可以看到,最优增益 $g_{\text{opt}}=\max\{g_{b_2|b_1}, g_{b_1|b_2}\}$ 的取值范围为 $\sqrt{2} \leq g_{\text{opt}} < 5$,此时的最优增益对应的是输出模Clone 1的最优增益,对于输出模Clone 2它不是最优的,并且当 $\eta_1=\eta_2$ 时, $g_{\text{opt}}=\sqrt{2}$,而当 $\eta_1 \neq \eta_2$ 时, $g_{\text{opt}}>\sqrt{2}$ 。

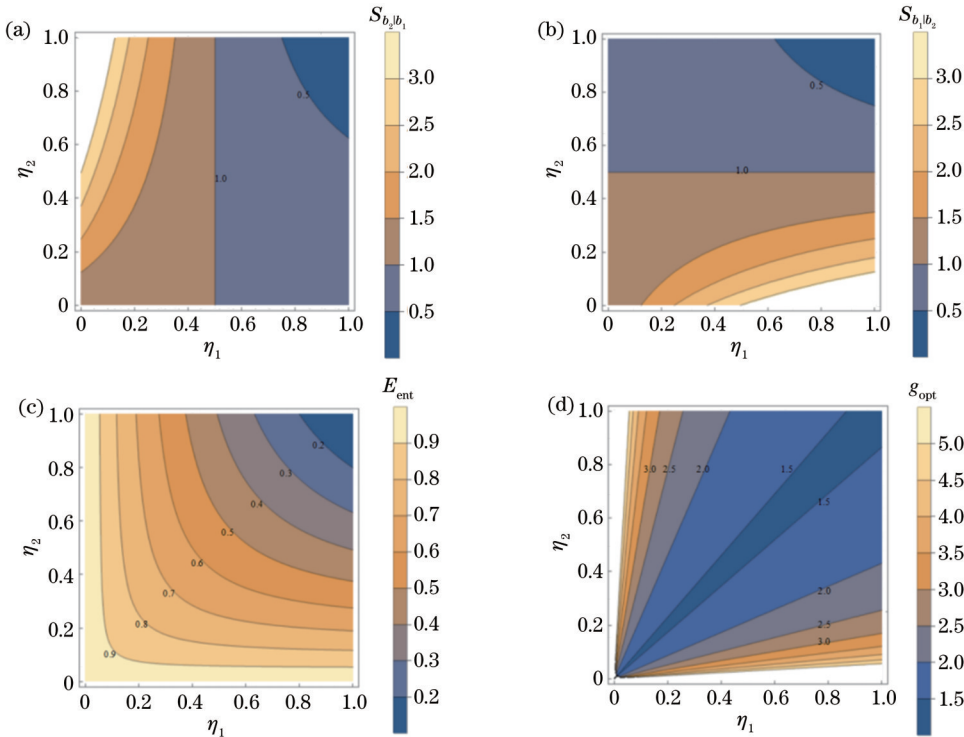


图2 纠缠源 \hat{b}_1 和 \hat{b}_2 之间的导引关系以及最优增益随 η_1 和 η_2 的变化($R=0.5$ 、 $r=1.15$)。(a) \hat{b}_1 对 \hat{b}_2 的导引随 η_1 和 η_2 的变化;(b) \hat{b}_2 对 \hat{b}_1 的导引随 η_1 和 η_2 的变化;(c) \hat{b}_1 和 \hat{b}_2 之间的纠缠随 η_1 和 η_2 的变化;(d)最优增益 g_{opt} 随 η_1 和 η_2 的变化

Fig. 2 Variation of the steering between entanglement sources \hat{b}_1 and \hat{b}_2 and optimal gain with η_1 and η_2 ($R=0.5$, $r=1.15$).
(a) Variation of steering of \hat{b}_2 by \hat{b}_1 with η_1 and η_2 ; (b) variation of steering of \hat{b}_1 by \hat{b}_2 with η_1 and η_2 ; (c) variation of entanglement between \hat{b}_1 and \hat{b}_2 with η_1 and η_2 ; (d) variation of the optimal gain with η_1 and η_2

4.2 取最优增益 g_{opt} 时,不同反射率下输出模Clone 1和Clone 2的保真度随 η_1 和 η_2 的变化

取 $r = 1.15$, $g_{\text{opt}} = \frac{|m-n| + \sqrt{(m-n)^2 + 4c^2}}{\sqrt{2} c \sqrt{\frac{1-R}{R}}}$ 是

可使输出模Clone 1保真度达到最大值的最优增益,但不是输出模Clone 2的最优增益。图3(a)~(c)给出了反射率 R 分别取0.3、0.5和0.7时输出模Clone 1的保真度随 η_1 和 η_2 的变化。当 $\eta_1 > 0.5$ 且 $\eta_2 > 0.5$ (图3(b))

中虚线以上区域)时, \hat{b}_1 和 \hat{b}_2 之间存在双向导引。从图3(a)~(c)可以得出,保真度 $F_1 > \frac{2}{3}$ 必然在该双向导引区域内,但是双向导引区域的保真度并不一定都满足 $F_1 > \frac{2}{3}$,并且输出模Clone 1的保真度随反射率的增加而减小。图3(d)~(f)展示了反射率分别取0.3、0.5和0.7时输出模Clone 2的保真度随 η_1 和 η_2 的变化。输出模Clone 2的保真度随反射率的增加而减小。因此,克隆过程中高保真度的实现不需要较高的反射率。

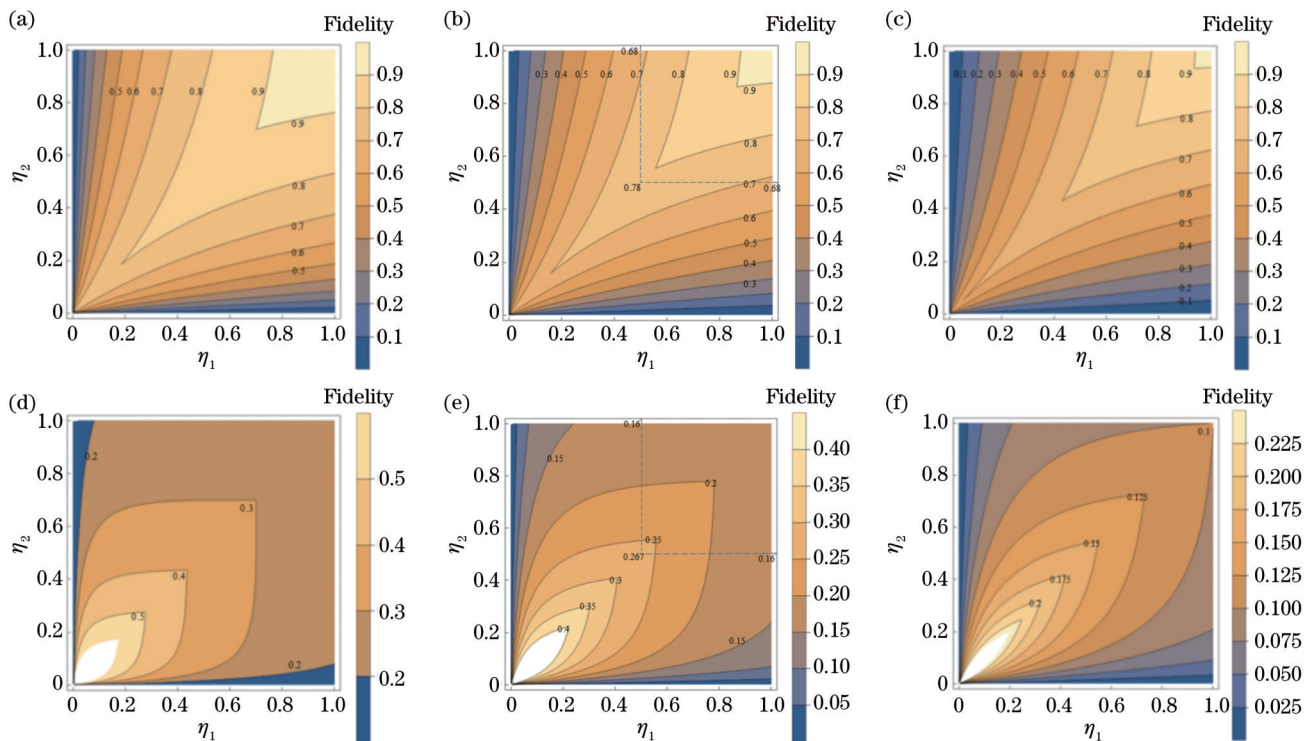


图3 $r = 1.15$ 时输出模Clone 1和Clone 2的保真度随 η_1 和 η_2 的变化。(a)~(c)反射率分别取0.3、0.5、0.7时Clone 1的保真度随 η_1 和 η_2 的变化;(d)~(f)反射率分别取0.3、0.5、0.7时Clone 2的保真度随 η_1 和 η_2 的变化

Fig. 3 Fidelity of output models Clone 1 and Clone 2 varies with η_1 and η_2 where $r = 1.15$. (a)–(c) Fidelity of Clone 1 varies with η_1 and η_2 when the reflectivity is 0.3, 0.5, and 0.7 respectively; (d)–(f) fidelity of Clone 2 varies with η_1 and η_2 when the reflectivity is 0.3, 0.5, and 0.7 respectively

4.3 取最优增益 g_{opt} 时,不同压缩参数下输出模Clone 1和Clone 2的保真度随 η_1 和 η_2 的变化

取 $R = 0.5$, $g_{\text{opt}} = \frac{|m-n| + \sqrt{(m-n)^2 + 4c^2}}{\sqrt{2} c \sqrt{\frac{1-R}{R}}}$,

图4(a)~(c)所示为压缩参数分别取 $r=0.35$ 、 $r=0.70$ 和 $r=1.15$ 时输出模Clone 1的保真度随 η_1 和 η_2 的变化,同样当 $\eta_1 > 0.5$ 且 $\eta_2 > 0.5$ [图4(c)中虚线以上区域]时, \hat{b}_1 和 \hat{b}_2 存在双向导引。从图4(a)~(c)可以看出,该双向导引区域内的保真度均大于 $\frac{2}{3}$,并且在较小的压缩参数下也可以通过双向导引来实现超越不

可克隆阈值的保真度。图4(d)~(f)所示为压缩参数分别取 $r=0.35$ 、 $r=0.70$ 和 $r=1.15$ 时输出模Clone 2的保真度随 η_1 和 η_2 的变化,可以看出,输出模Clone 2的保真度随压缩度的增加而减小。因此,使用较小纠缠但可导引的资源可以实现较高的克隆保真度。

5 结 论

基于部分脱体传输连续变量 $1 \rightarrow 2$ 量子克隆方案,理论研究了克隆保真度与EPR导引之间的关系,并深入探讨了克隆保真度在某一确定增益下随分束器反射率和压缩参数的变化。研究结果表明:对于输出模Clone 1,取最优增益时,克隆保真度超过不可克隆

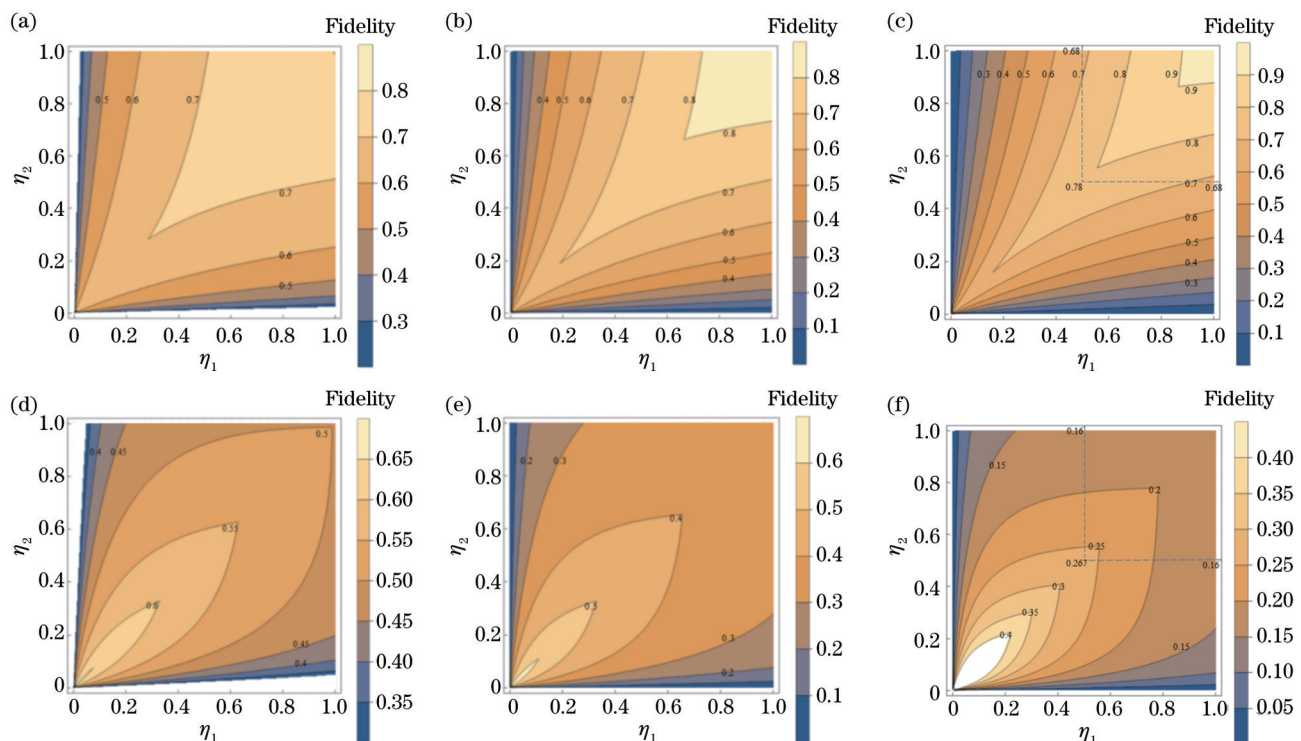


图4 $R = 0.5$ 时输出模Clone 1和Clone 2保真度随 η_1 和 η_2 的变化。(a)~(c)压缩参数分别取0.35、0.70、1.15时,Clone 1的保真度随 η_1 和 η_2 的变化;(d)~(f)压缩参数分别取0.35、0.70、1.15时,Clone 2的保真度随 η_1 和 η_2 的变化

Fig. 4 Fidelity of output models Clone 1 and Clone 2 varies with η_1 and η_2 where $R = 0.5$. (a)–(c) Fidelity of Clone 1 varies with η_1 and η_2 when the squeezing parameter is 0.35, 0.70, and 1.15 respectively; (d)–(f) fidelity of Clone 2 varies with η_1 and η_2 when the squeezing parameter is 0.35, 0.70, and 1.15 respectively

阈值需要共享纠缠源的双向导引,但并不是所有双向导引的资源都能使克隆的保真度大于 $\frac{2}{3}$;输出模

Clone 1的保真度随着反射率的增加和压缩参数的减小而减小,在较小的压缩参数下通过双向导引也能够实现保真度超越不可克隆阈值;与此同时,该增益下输出模Clone 2的保真度随着反射率的增加和压缩参数的增加而减小。因此,实现较高的克隆保真度不需要显著的压缩,也不需要较高的反射率。可以利用量子信道和经典信道相结合的方法来提高克隆的保真度,双向量子导引态是实现相干态安全量子克隆的必要资源。该研究结果可为量子通信网络的安全性提供一定的参考。

参 考 文 献

- [1] Einstein A, Podolsky B, Rosen N. Can quantum-mechanical description of physical reality be considered complete? [J]. Physical Review, 1935, 47(10): 777-780.
- [2] Schrödinger E. Discussion of probability relations between separated systems[J]. Mathematical Proceedings of the Cambridge Philosophical Society, 1935, 31(4): 555-563.
- [3] Reid M D. Demonstration of the Einstein-Podolsky-Rosen paradox using nondegenerate parametric amplification[J]. Physical Review A, 1989, 40(2): 913-923.
- [4] Jones S J, Wiseman H M, Doherty A C. Entanglement, Einstein-Podolsky-Rosen correlations, bell nonlocality, and steering[J]. Physical Review Letters, 2007, 98(13): 130402.
- [5] Bowles J, Vértesi T, Quintino M T, et al. One-way Einstein-Podolsky-Rosen steering[J]. Physical Review Letters, 2014, 112(20): 200402.
- [6] Wollmann S, Walk N, Bennet A J, et al. Observation of genuine one-way Einstein-Podolsky-Rosen steering[J]. Physical Review Letters, 2016, 116(16): 160403.
- [7] Sun K, Ye X J, Xu J S, et al. Experimental quantification of asymmetric Einstein-Podolsky-Rosen steering[J]. Physical Review Letters, 2016, 116(16): 160404.
- [8] 翟淑琴, 袁楠. 基于损耗和高斯噪声的连续变量多组分EPR导引操控[J]. 中国激光, 2021, 48(20): 2021001.
- [9] Zhai S Q, Yuan N. Manipulated multipartite continue-variable EPR steering with loss and Gaussian noise[J]. Chinese Journal of Lasers, 2021, 48(20): 2021001.
- [10] Xiang Y, Kogias I, Adesso G, et al. Multipartite Gaussian steering: monogamy constraints and quantum cryptography applications[J]. Physical Review A, 2017, 95(1): 010101.
- [11] Deng X W, Xiang Y, Tian C X, et al. Demonstration of monogamy relations for Einstein-Podolsky-Rosen steering in Gaussian cluster states[J]. Physical Review Letters, 2017, 118(23): 230501.
- [12] Branciard C, Cavalcanti E G, Walborn S P, et al. One-sided device-independent quantum key distribution: security, feasibility, and the connection with steering[J]. Physical Review A, 2012, 85(1): 010301.
- [13] 杨挪亚, 李崇. 量子导引在量子通讯中的作用[J]. 首都师范大学学报(自然科学版), 2022, 43(4): 33-37.
- [14] Yang N Y, Li C. Effect of quantum steering in quantum communication process[J]. Journal of Capital Normal University (Natural Science Edition), 2022, 43(4): 33-37.
- [15] Bennett C H, Brassard G, Crépeau C, et al. Teleporting an

- unknown quantum state via dual classical and Einstein-Podolsky-Rosen channels[J]. Physical Review Letters, 1993, 70(13): 1895-1899.
- [14] Furusawa A, Sørensen J L, Braunstein S L, et al. Unconditional quantum teleportation[J]. Science, 1998, 282(5389): 706-709.
- [15] Piani M, Watrous J. Necessary and sufficient quantum information characterization of Einstein-Podolsky-Rosen steering [J]. Physical Review Letters, 2015, 114(6): 060404.
- [16] Wootters W K, Zurek W H. A single quantum cannot be cloned [J]. Nature, 1982, 299(5886): 802-803.
- [17] Bužek V, Hillery M. Quantum copying: beyond the no-cloning theorem[J]. Physical Review A, 1996, 54(3): 1844-1852.
- [18] Zhu D, Shang W M, Zhang F L, et al. Quantum cloning of steering[J]. Chinese Physics Letters, 2022, 39(7): 070302.
- [19] Irvine W T M, Linares A L, de Dood M J A, et al. Optimal quantum cloning on a beam splitter[J]. Physical Review Letters, 2004, 92(4): 047902.
- [20] Fasel S, Gisin N, Ribordy G, et al. Quantum cloning with an optical fiber amplifier[J]. Physical Review Letters, 2002, 89(10): 107901.
- [21] Nagali E, Giovannini D, Marrucci L, et al. Experimental optimal cloning of four-dimensional quantum states of photons [J]. Physical Review Letters, 2010, 105(7): 073602.
- [22] Nagali E, Sansoni L, Sciarrino F, et al. Optimal quantum cloning of orbital angular momentum photon qubits through Hong-Ou-Mandel coalescence[J]. Nature Photonics, 2009, 3(12): 720-723.
- [23] Bouchard F, Fickler R, Boyd R W, et al. High-dimensional quantum cloning and applications to quantum hacking[J]. Science Advances, 2017, 3(2): e1601915.
- [24] Weedbrook C, Pirandola S, Garcia-Patrón R, et al. Gaussian quantum information[J]. Reviews of Modern Physics, 2012, 84(2): 621-669.
- [25] Cerf N J, Ipe A, Rottenberg X. Cloning of continuous quantum variables[J]. Physical Review Letters, 2000, 85(8): 1754-1757.
- [26] Andersen U L, Josse V, Leuchs G. Unconditional quantum cloning of coherent states with linear optics[J]. Physical Review Letters, 2005, 94(24): 240503.
- [27] Koike S, Takahashi H, Yonezawa H, et al. Demonstration of quantum telecloning of optical coherent states[J]. Physical Review Letters, 2006, 96(6): 060504.
- [28] Haw J Y, Zhao J, Dias J, et al. Surpassing the no-cloning limit with a heralded hybrid linear amplifier for coherent states[J]. Nature Communications, 2016, 7: 13222.
- [29] Grosshans F, Grangier P. Quantum cloning and teleportation criteria for continuous quantum variables[J]. Physical Review A, 2001, 64(1): 010301.
- [30] Yonezawa H, Aoki T, Furusawa A. Demonstration of a quantum teleportation network for continuous variables[J]. Nature, 2004, 431(7007): 430-433.
- [31] Yin J, Ren J G, Lu H, et al. Quantum teleportation and entanglement distribution over 100-kilometre free-space channels [J]. Nature, 2012, 488(7410): 185-188.
- [32] Wang K, Yu X T, Zhang Z C. Two-qubit entangled state teleportation via optimal POVM and partially entangled GHZ state[J]. Frontiers of Physics, 2018, 13(5): 130320.
- [33] Guo Y N, Tian Q L, Zeng K, et al. Fidelity of quantum teleportation in correlated quantum channels[J]. Quantum Information Processing, 2020, 19(6): 182.
- [34] 荆杰泰, 张凯, 刘胜帅. 基于原子系综四波混频过程的量子信息协议[J]. 光学学报, 2022, 42(3): 0327003.
- [35] Jing J T, Zhang K, Liu S S. Quantum information protocols based on four-wave mixing process in atomic ensemble[J]. Acta Optica Sinica, 2022, 42(3): 0327003.
- [36] 邢磊, 杨光, 聂敏, 等. 基于超纠缠中继的量子组播网络路由策略[J]. 激光与光电子学进展, 2023, 60(7): 0727001.
- [37] Xing L, Yang G, Nie M, et al. Routing protocol for quantum multicast networks based on hyperentangled relays[J]. Laser & Optoelectronics Progress, 2023, 60(7): 0727001.
- [38] Duan L M, Giedke G, Cirac J I, et al. Inseparability criterion for continuous variable systems[J]. Physical Review Letters, 2000, 84(12): 2722-2725.
- [39] Giovannetti V, Mancini S, Vitali D, et al. Characterizing the entanglement of bipartite quantum systems[J]. Physical Review A, 2003, 67(2): 022320.
- [40] Zhang T C, Goh K W, Chou C W, et al. Quantum teleportation of light beams[J]. Physical Review A, 2003, 67(3): 033802.

Secure Continuous Variable Quantum Cloning Based on EPR Steering

Wang Jun¹, Zhai Shuqin^{1,2*}

¹College of Physics and Electronic Engineering, Shanxi University, Taiyuan 030006, Shanxi, China;

²State Key Laboratory of Quantum Optics and Quantum Optics Devices, Institute of Opto-Electronics, Shanxi University, Taiyuan 030006, Shanxi, China

Abstract

Objective Quantum communication is based on the three principles of uncertainty, measurement collapse, and no-cloning in quantum mechanics. Compared with traditional classical communication methods, quantum communication features security and high efficiency and has great application significance and prospect in information security. In recent years, domestic and international scientists have conducted a lot of research on theories and experiments and made outstanding achievements in long-distance transmission and practical network of quantum communication. Quantum teleportation and quantum cloning have caught extensive attention as important protocols in quantum communication. With the help of quantum entanglement and classical communication, the transmission of any unknown quantum state from one location to another can be realized. As important resources of quantum information, quantum entanglement and EPR steering are widely adopted in various quantum communication tasks. The natural asymmetry of EPR steering makes

quantum steering a helpful resource in various quantum information processes. In the tasks of single-side device-independent quantum-key distribution, secure quantum teleportation, and subchannel discrimination, quantum steering can improve key acquisition rate, and enhance the protocol efficiency and security. In 2000, Cerf N J *et al.* proposed quantum cloning of Gaussian states with continuous variables and gave the fidelity boundary of quantum cloning as 2/3. In 2001, the Grangier P group presented the quantum and classical fidelity boundary of coherent state continuous variable quantum cloning under Heisenberg representation. For coherent state input, quantum teleportation is achieved when the fidelity exceeds the classical limit of 1/2, which is the best value that can be obtained without entanglement. However, it is necessary to have certain requirements for entangled beams to realize quantum teleportation with a fidelity greater than 2/3. In 2004, the Furusawa group applied three single-mode OPOs to obtain a continuous variable quantum teleportation network with an optimal fidelity of 0.64, and then they utilized four OPOs to achieve quantum teleportation with a fidelity of 0.7. In 2012, Pan J W group experimentally realized long-distance quantum teleportation. In 2018, Wei J H *et al.* put forward a quantum teleportation scheme using non-maximum entangled states for measurement. In 2018, Wang K *et al.* studied teleportation by partially entangled GHZ states. The analysis based on quantum cloning shows that for coherent state inputs, secure teleportation is guaranteed if the teleportation fidelity is greater than 2/3. To sum up, the research on remote transmission security is still a long-term important topic.

Methods Based on the basic idea of quantum teleportation, we employ the method of combining quantum channel and classical channel to design a 1→2 quantum cloning scheme with continuous variables by partially disembodied transport. The relationship between the fidelity of a partially disembodied transport cloning scheme and EPR entanglement source is studied theoretically. Firstly, the fidelity of two output modes in 1→2 cloning scheme, the entanglement and steering of EPR shared entanglement source are analyzed. Secondly, the relationship between the fidelity of the output mode Clone 1 and the steering characteristics under the optimal gain is studied. Thirdly, the fidelity of the output mode Clone 2 varies with the reflectance and squeezing parameters under the optimal gain of the output mode Clone 1.

Results and Discussions First, we analyze the variation of the steering between entanglement sources \hat{b}_1 and \hat{b}_2 and optimal gain with η_1 and η_2 . Only if $\eta_1 > 0.5$ there is a steering of \hat{b}_2 by \hat{b}_1 , and if $\eta_2 > 0.5$ there is a steering of \hat{b}_1 by \hat{b}_2 . The results are as follows: when $\eta_1 > 0.5$ and $\eta_2 > 0.5$, there is a two-way steering between \hat{b}_1 and \hat{b}_2 , and the entanglement amount between the sources increases with the improving transmission efficiency η_1 and η_2 . The range of optimal gain $g_{\text{opt}} = \max\{g_{b_2|b_1}, g_{b_1|b_2}\}$ is $\sqrt{2} \leq g_{\text{opt}} < 5$, and the optimal gain corresponds to the optimal gain of output mode Clone 1, which is not optimal for output mode Clone 2. Second, the fidelity of output modes Clone 1 and Clone 2 varies with η_1 and η_2 under different reflectance when the optimal gain g_{opt} is taken. The fidelity $F_1 > \frac{2}{3}$ should be in the two-way steering region, but the fidelity of the two-way steering region may not always meet $F_1 > \frac{2}{3}$. Meanwhile, the fidelity of output mode Clone 1 decreases with the increasing reflectivity, and that of output mode Clone 2 reduces with the rising reflectance. Third, the fidelity of output modes Clone 1 and Clone 2 varies with η_1 and η_2 under different squeezing parameters when the optimal gain g_{opt} is taken. The fidelity of output mode Clone 1 in the two-way steering region is greater than 2/3, and the fidelity beyond the no-cloning threshold can also be achieved by two-way steering under smaller squeezing parameters. The fidelity of the output mode Clone 2 decreases with the increase in squeezing parameters.

Conclusions In summary, we theoretically investigate the relationship between the fidelity of cloning and EPR steering based on the partially disembodied transport continuous variable 1→2 quantum cloning scheme. Meanwhile, we explore the fidelity variation with the reflectance of the beam-splitter and squeezing parameters at a given gain. The results show that for the output mode Clone 1, when the optimal gain is obtained, the two-way steering of the entanglement source should be shared when the fidelity exceeds the no-cloning threshold, but not all two-way steering resources can make the cloning fidelity greater than 2/3. The fidelity of output mode Clone 1 decreases with the rising reflectance and decreasing squeezing parameters, and the two-way steering can also achieve fidelity beyond the no-cloning threshold under smaller squeezing parameters. Additionally, the fidelity of the output mode Clone 2 reduces with the increasing reflectance and squeezing parameters. Therefore, high cloning fidelity does not require significant squeezing and high reflectivity. Therefore, we can employ the combination of quantum channel and classical channel to improve the cloning fidelity. The two-way quantum steering state is the necessary resource for secure quantum cloning of the coherent states. The research results provide certain references for the security of quantum communication networks.

Key words quantum optics; quantum cloning; quantum correlation; two-way steering